RESEARCH ARTICLE

Antiretroviral drug dolutegravir induces inflammation at the mouse brain barriers

Chang Huang | Md. Tozammel Hoque | Qing Rui Qu | Jeffrey Henderson | Reina Bendayan

Department of Pharmaceutical Sciences, Leslie Dan Faculty of Pharmacy, University of Toronto, Toronto, Ontario, Canada

Correspondence
Reina Bendayan, Department of Pharmaceutical Sciences, Leslie Dan Faculty of Pharmacy, University of Toronto, Toronto, ON, Canada.
Email: r.bendayan@utoronto.ca

Abstract

Integrase strand transfer inhibitors (INSTIs) based antiretroviral therapy (ART) is currently used as first-line regimen to treat HIV infection. Despite its high efficacy and barrier to resistance, ART-associated neuropsychiatric adverse effects remain a major concern. Recent studies have identified a potential interaction between the INSTI, dolutegravir (DTG), and folate transport pathways at the placental barrier. We hypothesized that such interactions could also occur at the two major blood–brain interfaces: blood-cerebrospinal fluid barrier (BCSFB) and blood–brain barrier (BBB). To address this question, we evaluated the effect of two INSTIs, DTG and bictegravir (BTG), on folate transporters and receptor expression at the mouse BCSFB and the BBB in vitro, ex vivo and in vivo. We demonstrated that DTG but not BTG significantly downregulated the mRNA and/or protein expression of folate transporters (RFC/*SLC19A1*, PCFT/*SLC46A1*) in human and mouse BBB models in vitro, and mouse brain capillaries ex vivo. Our in vivo study further revealed a significant downregulation in *Slc19a1* and *Slc46a1* mRNA expression at the BCSFB and the BBB following a 14-day DTG oral treatment in C57BL/6 mice. However, despite the observed downregulatory effect of DTG in folate transporters/receptor at both brain barriers, a 14-day oral treatment of DTG-based ART did not significantly alter the brain folate level in animals. Interestingly, DTG treatment robustly elevated the mRNA and/or protein expression of pro-inflammatory cytokines and chemokines (*Cxcl1, Cxcl2, Cxcl3, Il6, Il23, Il12*) in

Abbreviations: ABC, ATP-binding cassette; ART, antiretrovirals therapy; ARV, antiretroviral drug; BBB, blood–brain barrier; BCRP, breast cancer resistance protein; BCSFB, blood-cerebrospinal fluid barrier; BTG, bictegravir; CCL2, chemokine (C-C motif) ligand 2; CFD, cerebral folate deficiency; CNS, central nervous system; CP, choroid plexus; CSF, cerebrospinal fluid; CXCL1, chemokine (C-X-C motif) ligand 1; CXCL2, chemokine (C-X-C motif) ligand 2; DTG, dolutegravir; FRα, folate receptor alpha; FTC, emtricitabine; HAND, HIV-associated neurocognitive disorders; hCMEC/D3, immortalized cultures of human cerebral microvessel endothelial cells; HIV, human immunodeficiency virus; IL1β, interleukin – 1 beta; IL6, interleukin 6; iNOS, inducible nitric oxide synthase; INSTI, integrase strand transfer inhibitors; MRP1, multidrug resistance-associated protein 1; MRP4, multidrug resistance-associated protein 4; NPAE, neuropsychiatric adverse effect; NRTI, nucleoside/nucleotide reverse transcriptase inhibitor; NTD, neural tube defect; P-gp, P-glycoprotein; PB, peanut butter; PCFT, proton-coupled folate transporter; PLWH, people living with HIV; qPCR, quantitative polymerase chain reaction; RFC, reduced folate carrier; SLC, solute carrier; TAF, tenofovir alafenamide; TJ, tight junction; TNFα, tumor necrosis factor alpha; ZO-1, zonula occludens-1; 5-MTH, 5-methyltetrahydrofolate.

primary cultures of mouse brain microvascular endothelial cells (BBB). DTG oral treatment also significantly upregulated proinflammatory cytokines and chemokine (*Il6, Il1β, Tnfα, Ccl2*) at the BCSFB in mice. We additionally observed a downregulated mRNA expression of drug efflux transporters (*Abcc1, Abcc4*, and *Abcb1a*) and tight junction protein (*Cldn3*) at the CP isolated from mice treated with DTG. Despite the structural similarities, BTG only elicited minor effects on the markers of interest at both the BBB and BCSFB. In summary, our current data demonstrates that DTG but not BTG strongly induced inflammatory responses in a rodent BBB and BCSFB model. Together, these data provide valuable insights into the mechanism of DTG-induced brain toxicity, which may contribute to the pathogenesis of DTG-associated neuropsychiatric adverse effect.

1 | INTRODUCTION

Despite the implementation of combined antiretroviral therapy (ART), which has significantly reduced the mortality associated with human immunodeficiency virus (HIV) infection, people living with HIV (PLWH) present a high incidence of neuropsychiatric manifestations and cognitive deficits.[1] Side effects of antiretroviral drugs (ARVs), particularly neuropsychiatric symptoms, have been commonly reported with the use of ART without a clear knowledge of the underlying mechanism.[2] In recent years, emerging evidence also suggested an association between the use of ART and HIV-associated neurocognitive disorders (HAND).[3] Considering the lifelong requirement of ART treatment, it is essential to assess the potential toxicity of commonly used ARVs in the central nervous system (CNS).[4]

PLWH are particularly susceptible (~30%) to folate (vitamin B9) deficiency, with incidence being highest among those with neuropsychiatric effects.[5] Dolutegravir (DTG) or bictegravir (BTG) (integrase strand transfer inhibitors (INSTI)) – based ART, usually administered with a nucleoside/nucleotide reverse transcriptase inhibitor (NRTI) backbone of tenofovir alafenamide and emtricitabine, are the current recommended first-line therapy owing to their great potency, high barrier to resistance, and tolerability.[6] However, safety concerns such as high incidence of neuropsychiatric adverse effect (NPAEs) have been reported.[7] The 2018 Botswana surveillance study identified an increased risk of neural tube defects (NTD) associated with DTG exposure at conception.[8] Given that maternal folate deficiency is the primary risk factor for NTD, several preclinical studies were conducted to investigate the potential DTG-mediated alteration of folate transport at the placental-fetal barrier, revealing a potential inhibitory effect of DTG on folate transporters/receptor.[9,10]

Developmentally folate is an essential micronutrient that plays an critical role in one carbon metabolism, thus affecting cellular functions including biosynthesis of nucleic acid, amino acid homeostasis, epigenetics, and redox defense.[11] Additionally folate is critical for brain health across all age groups in part due to its maintenance of S-adenosylmethionine, the high energy methyl donor essential for transsulfuration reactions maintaining cysteine/glutathione stores, drug (detoxification) and DNA (epigenetic) methylation reactions; as well as synthesis of neurotransmitters.[12] Consistent with this, cerebral folate deficiency (CFD) is linked to multiple adverse outcomes including developmental delays, seizures, and progressive ataxia.[13] Neurological and psychiatric conditions including depression, dementia, and demyelinating myelopathy have also been reported as a result of CFD.[14] In addition to vitamin deficiency, inborn errors of metabolism such as deficiencies of enzymes (e.g. dihydrofolate reductase) and defects in cerebral folate transport represent the primary causes of CFD.[15] Pathological conditions such as metabolic disease, immune alteration, and effects of drugs can be the secondary causes.[13] Although the precise mechanism of such pathogenic effects remains unclear, elevation of pro-inflammatory markers such as interleukin-6 (IL-6), interleukin-8 (IL-8), and interferon-γ (IFN-γ) is commonly associated with reductions in

5-methyltetrahydrofolate (5-MTHF) within the cerebrospinal fluid (CSF).[16–18]

Folate transport into the mammalian brain is primarily mediated by several members of the solute carrier (SLC) superfamily of membrane-associated transporters; reduced folate carrier (RFC/*SLC19A1*) and proton-coupled folate transporter (PCFT/*SLC46A1*), as well as folate receptor alpha (FRα/*FOLR1*).[19] Cerebral transfer of folates occurs actively at blood–brain interfaces, primarily at the choroid plexus (CP) but also at the blood–brain barrier (BBB).[20,21] Studies suggest that FRα expressed along the basolateral (plasma) side of the CP mediates endocytosis of folates. This process is coupled through acidic endosome formation and subsequent exocytosis to the CSF via FRα located at the apical (CSF) side of the CP.[22] The PCFT transporter is mainly found in intracellular compartments colocalized with FRα, and is responsible for folate transport out of acidified endosomes into the cytoplasm.[23] FRα and PCFT are thus crucial to cerebral folate delivery, as demonstrated in human subjects developing CFD with loss-of-function mutations to either FRα or PCFT.[24] RFC, a bidirectional transporter, is proposed to transport folates into the CSF by a saturable mechanism at the CP apical surface.[25] In comparison, due to the lack of FRα expression at the microvasculature endothelium (BBB) in humans, RFC and PCFT are considered the major players in transporting folate and folate derivatives such as 5MTHF at the microvasculature endothelium as previously demonstrated by our group and others.[25–29]

The CP epithelium is the major source of CSF production, providing the brain with an auxiliary protection from the periphery in addition to the BBB.[30,31] Similar to the BBB, the expression of tight junction (TJ) proteins includes zonula occludens-1 (ZO-1), occludin and claudins (Cldn1, Cldn3) between adjacent cells at the CP epithelium, strictly regulating paracellular access of ions and macromolecules.[32] Efflux transporters, particularly the multidrug resistant proteins MRP1 and MRP4, are highly expressed along the basolateral membrane of the CP, further limiting the passage of xenobiotics.[33] P-glycoprotein (P-gp) and Breast Cancer Resistant Protein (BCRP) are expressed along the apical side of the CP epithelium.[33–35] Importantly, in addition to its physical and biochemical barrier features, the CP is considered as an immunological niche of the CNS by housing various types of immune cells such as macrophages, T cells, and dendritic cells within the stroma.[31,36] Owing to the secretory function of the CP, this tissue is essential in relaying inflammatory signals to the CNS via the release of inflammatory factors such as IL6, IL1β, TNFα, and others into the CSF.[36] As such, the CP has been shown to play a pivotal role in the pathogenesis of cerebral infection,

immune dysregulation, and micronutrient transport defects in the brain.[37,38] Notably, the inflammatory response has been shown to be closely associated with loss of TJ barrier function and transporter dysregulation, as reported by others in various sites including astrocytes, intestinal barrier, and BBB.[39–41]

Considering the prevalence of HIV-associated CNS complications associated with the lifelong use of ART, it is essential to evaluate any potential toxicity of commonly used ARVs in the CNS. Given that DTG has been previously reported to elicit inflammatory responses in several cell-based systems,[42,43] and inhibit folate transport at the placental-fetal barrier,[9,44] we investigated its effects at the CP and BBB. BTG, a second generation INSTI that was structurally derived from DTG, was also investigated due to its potential for such effect.[45] Specifically, we assessed DTG and BTG for their ability to trigger inflammation and dysregulate folate transporters/receptor, ABC transporters, and tight junction proteins at the CP and BBB, using in vitro, ex vivo, and in vivo models.

2 | METHODS

2.1 | Reagents/materials

All cell culture reagents were of highest purity and obtained from Invitrogen (Carlsbad, CA, USA), unless indicated otherwise. Real-time quantitative polymerase chain reaction (qPCR) reagents, including reverse transcription cDNA kits and qPCR TaqMan primers, were purchased from Applied Biosystems (Foster City, CA, USA) and Life Technologies (Carlsbad, CA, USA), respectively. qPCR FastMix was purchased from Quantabio (Beverly, MA, USA). All buffers were purchased from Sigma-Aldrich (Oakville, ON, CA). Ficoll (Polysucrose 400) was obtained from BioShop (Burlington, ON, CA) and PluriStrainer 30 μm was purchased from PluriSelect Life Science (EI Cajon, CA, USA). 3-(4,5-dimethylthiazol-2-yl)-2,5-diphenyltetrazolium bromide (MTT), primary rabbit polyclonal anti-SLC19A1 (RFC; AV44167), and anti-SLC46A1 (PCFT; SAB2108339) antibodies were purchased from Sigma-Aldrich (Oakville, ON, Canada). Mouse monoclonal anti-β actin (sc-47778) antibody was obtained from Santa Cruz Biotechnology (Dallas, TX, USA). Anti-rabbit or anti-mouse horseradish peroxidase-conjugated secondary antibodies and all ARVs (DTG, BTG, TAF, and FTC) were purchased from Cedarlane Laboratories (Burlington, ON, Canada). The LEGEND MAX™ Mouse IL-6 ELISA Kit (431307), LEGEND MAX™ Mouse IL-23 (p19/p40) ELISA Kit (433707), and LEGEND MAX™ Mouse IL-12 (433607) were purchased from BioLegend (San Diego, CA,

USA). A mouse MIP-2 /CXCL2 ELISA Kit (RAB0128) was purchased from Sigma-Aldrich (Oakville, ON, Canada).

2.2 | Cell cultures

Immortalized human cerebral microvessel endothelial cell line (hCMEC/D3), an established model of human BBB[46] was generously provided by P.O. Couraud (Institut Cochin, Department Biologie Cellulaire and INSERM, Paris, France); primary cultures of mouse microvascular endothelial cells were kindly provided by Dr. Isabelle Aubert (University of Toronto, ON, Canada). hCMEC/D3 cells (passage 29–36) were cultured in Endothelial Cell Basal Medium-2 (Lonza, Walkersville, MD, USA), supplemented with vascular endothelial growth factor, insulin-like growth factor 1, epidermal growth factor, fibroblast growth factors, hydrocortisone, ascorbate, GA-1000, heparin, and 2.5% fetal bovine serum (FBS), and grown on rat tail collagen type I-coated plates. Primary cultures of mouse (C57BL/6) brain microvascular endothelial cells were cultured (passage 2–6) in complete Mouse Endothelial Cell Medium (Cell Biologics Inc, Chicago, IL, USA), supplemented with vascular endothelial growth factor, endothelial cell growth supplements, heparin, epidermal growth factor, hydrocortisone, L-glutamine, antibiotic-Antimycotic Solution, and 5% FBS, and grown on gelatin-coated plates. All cell lines were maintained in a humidified incubator at 37°C with 5% CO_2 and 95% air atmosphere with fresh medium replaced every 2–3 days. Cells were sub-cultured with 0.25% trypsin–EDTA upon reaching 95% confluence prior to ARV treatment.

2.3 | Cell viability assay

Cell viability of hCEMC/D3 cells and primary cultures of mouse brain microvascular endothelial cells in the presence of DTG or BTG (1000–10 000 ng/mL) was assessed using the MTT assay. Following 24 h of treatment, cells were incubated for 2 h at 37°C with a 2.5 mg/mL MTT solution in PBS. The formazan content in each well was dissolved in DMSO and quantified by UV analysis at 580 nm using a SpectraMax 384 microplate reader (Molecular Devices, Sunnyvale, CA). Cell viability was assessed by comparing the absorbance of cellular reduced MTT in ARV-treated cells to that of vehicle (DMSO)-treated cells.

2.4 | Mouse brain capillary isolation

Brain capillaries were isolated from male C57BL/6 (9–10 weeks old) mice purchased from Charles River Laboratories (Laval, QC, Canada) as described previously by our laboratory.[47] Briefly, animals were anesthetized by isoflurane inhalation and decapitated once a deep anesthetic surgical plane was achieved. Brains were collected immediately, cortical gray matter was removed and homogenized in ice-cold isolation buffer (phosphate-buffered saline (PBS) containing calcium and magnesium, and supplemented with 5 mM glucose and 1 mM sodium pyruvate). Ficoll solution (30% final concentration) was added to the brain homogenates, mixed vigorously and centrifuged at 5800g for 20 min at 4°C. The resulting pellet of capillaries was re-suspended in 1% bovine serum albumin (BSA) and filtered through a 300 μm nylon mesh. The filtrate containing the capillaries was passed through a 30 μm PluriStrainer and washed with 20 mL PBS containing 1% BSA. Capillaries were harvested with 50 mL ice-cold isolation buffer and centrifuged at 1600g for 10 min. The resulting pellet containing the capillaries was snap-frozen in liquid nitrogen and kept at −80°C until further analysis. All experiments, procedures, and animal care were conducted in accordance with the Canadian Council on Animal Care guidelines and approved by the University of Toronto Animal Care Committee.

2.5 | Mouse CP tissue isolation

CP tissue was isolated from adult male C57BL6/N mice (9–10 weeks old). Animals were decapitated, and brains were immediately removed. Isolated brains were placed under a stereomicroscope in ice-cold isolation buffer (PBS containing calcium, magnesium, and supplemented with 5 mM glucose and 1 mM sodium pyruvate), with intact CP tissues removed from the lateral, third, and fourth ventricle and processed for further analysis.

2.6 | Gene expression analysis

The mRNA expression of genes of interest was quantified using qPCR. Total RNA was isolated from cell samples (hCMEC/D3, primary cultures of mouse brain microvascular endothelial cells), isolated mouse brain capillaries and isolated mouse CP tissue using TRIzol reagent (Invitrogen) and treated with DNase I to remove contaminating genomic DNA. RNA concentration (absorbance at 260 nm) and purity (absorbance ratio 260/280) were assessed using NanoDrop One Spectrophotometer (Thermo Scientific). A total amount of 2 μg of RNA was then reverse transcribed to cDNA using a high-capacity reverse transcription cDNA kit (Applied Biosystems) according to the manufacturer's instructions. Specific human or mouse primer for *SLC19A1/Slc19a1* (RFC/Rfc;

Hs00953344_m1/Mm00446220_m1), *SLC46A1/Slc46a1* (PCFT/Pcft; Hs00560565_m1/Mm00546630_m1), *Folr1* (Frα; Mm00433355_m1), *Il6* (Il6; Mm00446190_m1), *Il1β* (Il1β; Mm00434228_m1), *Ccl2* (Ccl2; Mm00441242_m1), *Nos2* (iNos; Mm00440502_m1), *Cxcl1* (Cxcl1; Mm04207460_m1), *Cxcl2* (Cxcl2; Mm00436450), *Cxcl3* (Cxcl3; Mm01701838), *Il23a* (Il23a; Mm00518984), *Il12b* (Il12b, Mm01288989), *Abcc1* (Mrp1; Mm00456156_m1), *Abcc4* (Mrp4; Mm01226381_m1), *Tjp1* (Zo-1; Mm01320638_m1), *Ocln* (Ocln; Mm00500912_m1), *Cldn1* (Cldn1; Mm01342184_m1), *Cldn3* (Cldn3; Mm00515499_s1); *Abcc1* (Mrp1; Mm00456156_m1), *Abcc4* (Mrp4; Mm01226381_m1), *Abcb1a* (P-gp; Mm00440761_m1), and *Abcg2* (Bcrp; Mm00496364_m1) were designed and validated by Life Technologies for use with TaqMan qPCR chemistry. All assays were performed in triplicates with the housekeeping gene for human/mouse cyclophilin B (PPIB/Ppib; Hs00168719_m1/Mm00478295_m1), or mouse glyceraldehyde-3-phosphate dehydrogenase (*Gapdh*; Mm99999915_g1) as an internal control. For each gene of interest, the critical threshold cycle (CT) was normalized to *PPIB//Ppib* or *Gapdh* using the comparative CT method. The difference in CT values (ΔCT) between the target gene and *PPIB/Ppib* or *Gapdh* was then normalized to the corresponding ΔCT of the vehicle control (ΔΔCT) and expressed as fold expression ($2^{-\Delta\Delta CT}$) to assess the relative difference in mRNA expression for each gene.

2.7 | Western blot analysis

Western blot analysis was performed according to our published protocol with minor modifications.[48] Briefly, cell lysates of hCMEC/D3 cells and primary cultures of mouse brain microvascular endothelial cells were obtained using a modified RIPA buffer [50 mM Tris pH 7.5, 150 mM NaCl, 1 mM EGTA, 1 mM sodium o-vanadate, 0.25% (v/v) sodium deoxycholic acid, 0.1% (v/v) sodium dodecyl sulfate (SDS), and 1% (v/v) NP-40, 200 μM PMSF, 0.1% (v/v) protease inhibitor]. Protein concentration of the lysates was quantified using Bradford's protein assay (Bio-Rad Laboratories) with BSA as the standard. Total protein (50 μg) for each sample was mixed in Laemmli buffer and 10% β-mercaptoethanol, separated on 10% SDS-polyacrylamide gel, and electro-transferred onto a polyvinylidene fluoride membrane overnight at 4°C. The blots were blocked for 1 h at room temperature in 5% skim milk Tris-buffered saline solution containing 0.1% Tween 20 and incubated with primary rabbit polyclonal anti-SLC19A1 (RFC) antibody (1:250), rabbit polyclonal anti-SLC46A1 (PCFT) antibody (1:250), and murine monoclonal anti-β-actin antibody (1:1000)

overnight at 4°C. The blots were incubated for 1.5 h with corresponding horseradish peroxidase-conjugated anti-rabbit (1:5000) or anti-mouse (1:5000) secondary antibody. Protein bands were detected using an enhanced chemiluminescence SuperSignal West Pico System (Thermo Fisher Scientific) and autoradiographed onto X-ray film.

2.8 | Quantification of cytokines and chemokines using enzyme-linked immunosorbent assay (ELISA)

Primary cultures of mouse brain microvascular endothelial cell were treated with either DMSO (vehicle control), DTG (2000 ng/mL, 5000 ng/mL) or BTG (3000 ng/mL, 6000 ng/mL) for 24 h at 37°C. Following the treatment, cell culture supernatants were collected, centrifuged at 1500 rpm at 4°C for 10 min and stored at −80°C until the day of analysis. The levels of Il6, Il23, Il12, Cxcl2 in the cell culture supernatant were quantified by LEGEND MAX™ Mouse IL-6, IL-23 (p19/p40) and IL-12 ELISA Kits and Mouse MIP-2/CXCL2 ELISA Kit as per manufacturer's instructions. Each kit consists of a 96-well strip plate that is pre-coated with specific antibodies that were used to investigate the levels of Il6, Il23, Il12 and Cxcl2. Absorbance was read at 450 nm using a SpectraMax 384 microplate reader (Molecular Devices, Sunnyvale, CA).

2.9 | In vitro and ex vivo ARV treatment

Confluent hCMEC/D3 or primary mouse brain microvascular endothelial cell monolayers at a density of 1.0×10^6/well grown on 6-well plates or T75 flasks were treated with either DMSO (vehicle control), DTG (2000 ng/mL, 5000 ng/mL) or BTG (3000 ng/mL, 6000 ng/mL) for a period of 24 h or 48 h at 37°C. Isolated mouse brain capillaries resuspended in 10 mL isolation buffer were also exposed to DMSO (vehicle control), DTG (5000 ng/mL) or BTG (6000 ng/mL) for 5 h at room temperature. Doses of ARVs were chosen to correspond to human therapeutic plasma levels.[49,50] At the desired time interval, treated cells or brain capillaries were harvested using TRIzol lysis buffer or modified RIPA buffer and processed for subsequent gene and protein analyses, respectively.

2.10 | In vivo ARV treatment

Wild-type male C57BL/6 (9-10-week-old) mice were purchased from Charles River Laboratories (Laval, QC,

Canada). DTG, BTG, and backbone ARVs: tenofovir alafenamide (TAF) and emtricitabine (FTC) in powder form were added to peanut butter (PB) and mixed by hand with a spatula for 10 min to make a homogenous suspension. PB pellets (100.5 ± 1.5 mg in weight) were made to formulate the concentration of the drug that was equivalent to DTG at 5 mg/kg/day; BTG at 5 mg/kg/day or vehicle control for study 1; TAF/FTC at 5/33.3 mg/kg/day; DTG + TAF/FTC at 5 + 5/33.3 mg/kg/day; BTG + TAF/FTC at 5 + 5/33.3 mg/kg/day or vehicle control for study 2. Doses of ARVs were chosen to achieve human therapeutic plasma levels in mice as previously reported.[51] Frozen pellets were then stored at −80°C until use. Each mouse was single-housed and was introduced to the taste of PB once daily for 5 consecutive days before the initiation of ARV treatment. After 5 days of training, the average pellet consumption time was ≤1 min. During the treatment, each mouse was dosed once daily at 10:00 am with one regular pellet (vehicle control) or drug-containing pellet for 14 days. At 24 h following the last PB pellet administration, mice were subjected to capillary isolation and CP tissue isolation for gene expression measurement (study 1) or were perfused and subjected to brain collection for subsequent quantification of folate levels applying the microbiological assay (study 2).

2.11 | Sample extraction, tri-enzyme extraction and folate microbiological assay

Brains were isolated 24 h after the last PB pellet administration and were snap frozen in 1% sodium ascorbate to prevent oxidation of folates. Briefly, the frozen samples were diluted x20 and homogenized in Wilson-Horne buffer (2% sodium ascorbate in 50 mM Hepes, 50 mM N-cyclohexyl-2-aminoethanesulfonic acid, and 0.2 M 2-mercaptoethanol [pH 7.85]) and divided into 0.5-mL aliquots. A mixture of sample extract (0.5 mL), protease (0.5 mL), and phosphate buffer (1 mL with 1% sodium ascorbate [pH = 4.1]) was incubated in a light-shielded water bath at 37°C for 2 h. Following the incubation, the samples were boiled at 100°C for 10 min to inactivate the protease and cooled on ice following the addition of α-amylase (0.3 mL), rat serum conjugase (0.25 mL) and phosphate buffer (1 mL with 1% sodium ascorbate [pH = 6.8]). The samples were then subsequently incubated at 37°C for 2 h and centrifuged at 5000 × g for 10 min.[26] The supernatant was collected and stored at −80°C until folate microbiological assay. The folate microbiological assay was performed with the assistance of Dr. Suzanne Aufreiter, in the Department of Nutritional Sciences, University of Toronto, as described by Horne.[52] Briefly the sample was diluted with 5 mg/mL sodium ascorbate and was added to a 96-well microplate with assay medium containing chloramphenicol-resistant Lactobacillus

rhamnosus and all the nutrients necessary for the growth of *L. rhamnosus*, except for folate. The plate was then incubated for 45 h at 37°C, and the total folate concentration was assessed by measuring the turbidity of the inoculated medium at 590 nm in a PowerWave microplate reader (Bio-Tek Instrument). For each run, a standard growth curve of the organisms was carried out. Three replicates were run for each sample to ensure the generation of accurate results. The calibration curve for this assay was generated using 5-methyltetrahydrofolate. Certified pig liver (13.3 mg folate/kg; Pig Liver, BCR 487, IRMM, Geel, Belgium) was used to assess the accuracy and reproducibility of the assay.[52]

2.12 | Data analysis

In vitro experiments were repeated 3–5 times with cells obtained from different passages. In each individual experiment, each experimental point was repeated at least 3 times. Ex vivo experiments with isolated mouse brain capillaries were repeated separately 3 times. In each individual experiment, the brain capillaries were pooled from 6 animals per treatment group ($n = 18$/group). The in vivo experiments with isolated mouse brain capillaries and CP tissues were repeated separately two times. The brain capillaries were isolated and pooled from 6 animals' brain tissues per treatment group (total $n = 12$, 2 pools of 6 subjects) from two independent experiments. The mouse CP tissues were pooled from 3 animals per treatment group (total $n = 12$; 4 pools of 3 subjects) from two independent experiments. For the in vivo study 2 assessing brain folate levels by the microbiological assay, the samples were collected from 5 animals per treatment group. Results are presented as mean ± SEM. All statistical analyses were performed using Prism 6 software (GraphPad Software Inc., San Diego, CA, USA). Statistical significance between two groups was assessed by two-tailed Student's *t* test for unpaired experimental values. Multiple group comparisons were performed using one-way analysis of variance (ANOVA) with Bonferroni's post-hoc test. $p < .05$ was considered statistically significant.

3 | RESULTS

3.1 | Effects of DTG and BTG on cell viability

Examination via MTT assay confirmed that the viability of hCMEC/D3 cells and primary cultures of mouse brain microvascular endothelial cells was not significantly affected by DTG (1000–10 000 ng/mL) or BTG (1000–8000 ng/mL) (Figure S1).

3.2 | Effects of ARVs on folate transporters/receptor expression in vitro in hCMEC/D3 cells and in primary cultures of mouse brain microvascular endothelial cells

To examine the effect of first line INSTIs on folate transporters in human BBB in vitro, hCMEC/D3 cells were exposed to DTG at 2000 ng/mL or 5000 ng/mL and BTG at 3000 ng/mL or 6000 ng/mL for 24 and 48 h to assess potential changes at the mRNA and protein level. At 5000 ng/mL DTG significantly downregulated *SLC19A1* and *SLC46A1* mRNA expression by ~20% and ~30%, respectively (Figure 1A). The dominant form of PCFT protein was detected in hCMEC/D3 at 63 kDa. Consistent with this, Western blot densitometric analysis revealed a significant decrease in the protein expression of the major glycosylated form of PCFT (63 kDa) in hCMEC/D3 cells treated with DTG at 2000 ng/mL or 5000 ng/mL, whereas RFC protein expression remained unchanged following DTG or BTG treatment (Figure 1B). BTG at 3000 ng/mL induced a modest but significant upregulation of both *SLC19A1* and *SLC46A1* mRNA expression (Figure 1A). However, these mild changes at the mRNA expression did not translate at the protein level (Figure 1B). As anticipated, *FOLR1* mRNA expression was undetectable in hCMEC/D3 cells. These findings are consistent with previous reports documenting the lack of this receptor at the human BBB.[53]

To examine the effect of first line INSTIs on folate transporter's expression in mouse BBB in vitro, primary cultures of mouse microvascular endothelial cells were exposed to DTG at 2000 ng/mL or 5000 ng/mL and BTG at 3000 ng/mL or 6000 ng/mL for 24 and 48 h to assess changes at the mRNA and protein level. We observed a significant and robust downregulation of *Slc19a1* (~40%) and *Slc46a1* (~80%) mRNA expression with DTG at 5000 ng/mL, however, no change was observed following BTG treatment (Figure 2A). *Folr1* mRNA expression was barely detectable in primary cultures of mouse brain microvascular endothelial cells and was not further investigated. The densitometric analysis further revealed a consistent and significant decrease in Rfc protein expression with DTG at 5000 ng/mL (Figure 2B). Strikingly, though we observed a robust downregulation of *Slc46a1* gene expression by DTG at 5000 ng/mL, no such change was observed at the protein level (Figure 2B). Instead, our immunoblotting data revealed a mild but significant decrease in Pcft protein expression following DTG treatment at 2000 ng/mL (Figure 2B). BTG treatment did not result in any significant changes on protein expression of Rfc or Pcft (Figure 2B).

3.3 | Effects of DTG and BTG on folate transporters/receptor expression ex vivo in isolated mouse brain capillaries

The effect of DTG and BTG on folate transporters/receptor at the BBB was additionally investigated ex vivo in isolated mouse brain capillaries following 5h exposure at room temperature. Exposure to DTG at 5000 ng/mL induced a significant reduction (~50%) in mRNA expression of *Slc19a1, Slc46a1*, and *Folr1* (Figure 3A). BTG treatment at 6000 ng/mL did not significantly alter the mRNA expression of *Slc46a1* and *Folr1*, whereas a ~30% downregulation of *Slc19a1* mRNA expression was observed following the 5h treatment (Figure 3B).

3.4 | In vivo effects of DTG and BTG chronic exposure on folate transporters/receptor expression at the CP and brain capillaries isolated from C57BL/6 mice
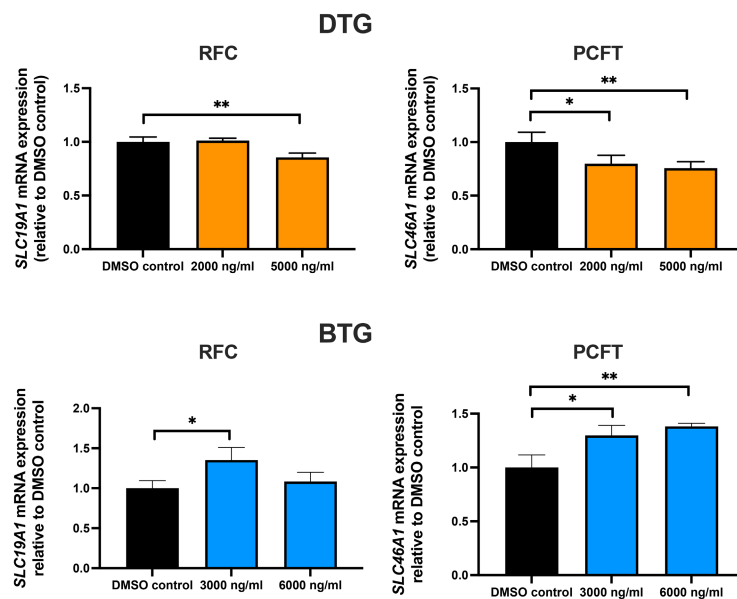
To further investigate the chronic effect of DTG or BTG on cerebral folate delivery pathways in vivo we next sought to quantify mRNA expression of folate transporters/receptor (*Slc19a1, Slc46a1, Folr1*) at the CP tissue and brain capillaries isolated from C57BL/6 mice orally treated with PB pellets containing DTG (5 mg/kg/day), BTG (5 mg/kg/day) or with the vehicle control (PB pellets with no drug) for 14 days.

DTG chronic treatment resulted in a modest but significant decrease in both *Slc19a1* (~25%) and *Slc46a1* (~25%) mRNA expression with no change in *Folr1* expression at the mouse CP. In comparison, we did not observe any significant alteration of folate transporters/receptor following BTG treatment (Figure 4A). DTG treatment additionally modestly but significantly reduced *Slc19a1* mRNA expression (~15%) and induced a more robust downregulation in *Slc46a1* (~40%) and *Folr1* (~25%) mRNA expression in mouse brain capillaries. BTG, on the other hand, had no effect on folate transporters, but modestly downregulated *Folr1* mRNA expression (~25%) at a comparable level as DTG in mouse brain capillaries (Figure 4B).

3.5 | In vivo effects of DTG and BTG chronic exposure on cerebral folate levels in C57BL/6 mice

To examine the effect of DTG and BTG on cerebral folate delivery, we treated the animals with the first line NRTIs backbone (TAF/FTC) with DTG and/or BTG, to better
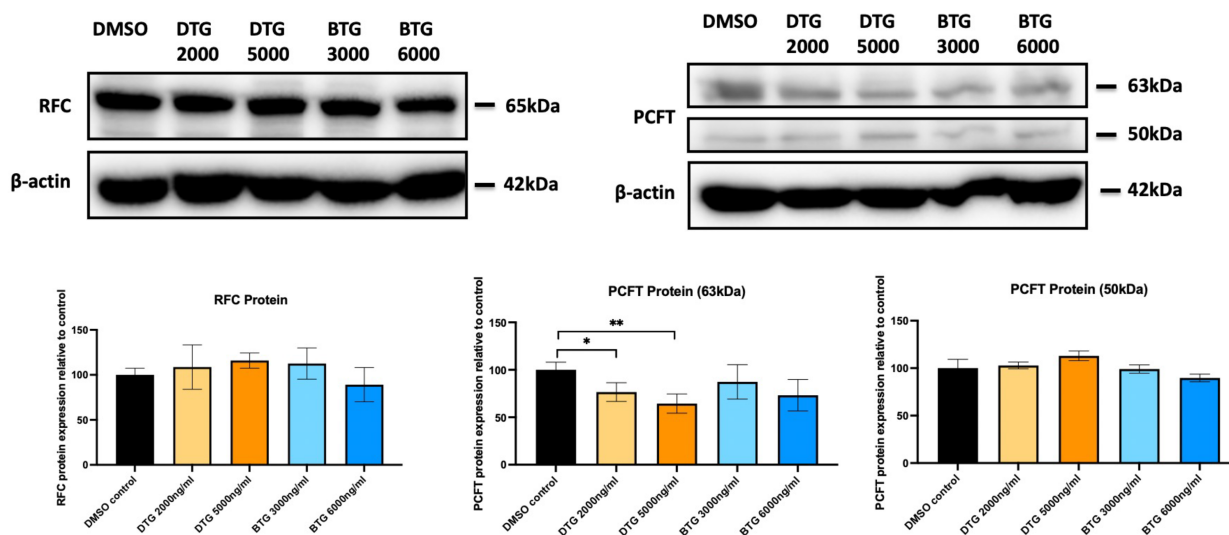
FIGURE 1 mRNA and protein expression of folate transporters in hCMEC/D3 cells exposed to DTG (2000 ng/mL, 5000 ng/mL) or BTG (3000 ng/mL, 6000 ng/mL) or vehicle (DMSO) control for 24 h and 48 h. (A) mRNA expression of *SLC19A1* and *SLC46A1* in cells exposed to INSTIs relative to vehicle (DMSO) control was assessed by qPCR. Results are presented as mean relative mRNA expression ± SEM normalized to the housekeeping human cyclophilin B gene from $n=4$ independent experiments. (B) Protein expression of RFC and PCFT was assessed by immunoblotting analysis, using specific antibodies as described in the methods section. β-Actin was used as a loading control. Representative blots and densitometric analysis are shown. Results are presented as mean relative protein expression ± SEM normalized to the DMSO control from $n=3$ independent experiments. One-way ANOVA with Bonferroni's post-hoc test analysis was applied, *$p<.05$; **$p<.01$.

reflect the ARV regimen used in the clinic. A backbone only group (without the co-administration of DTG or BTG) was included to better characterize the effect of DTG or BTG from the three-drug regimens. The data from

the microbiological assay did not reveal any significant changes of the cerebral folate levels between the groups following the 14-day ARV treatment in C75BL/6 mice (Figure 5).
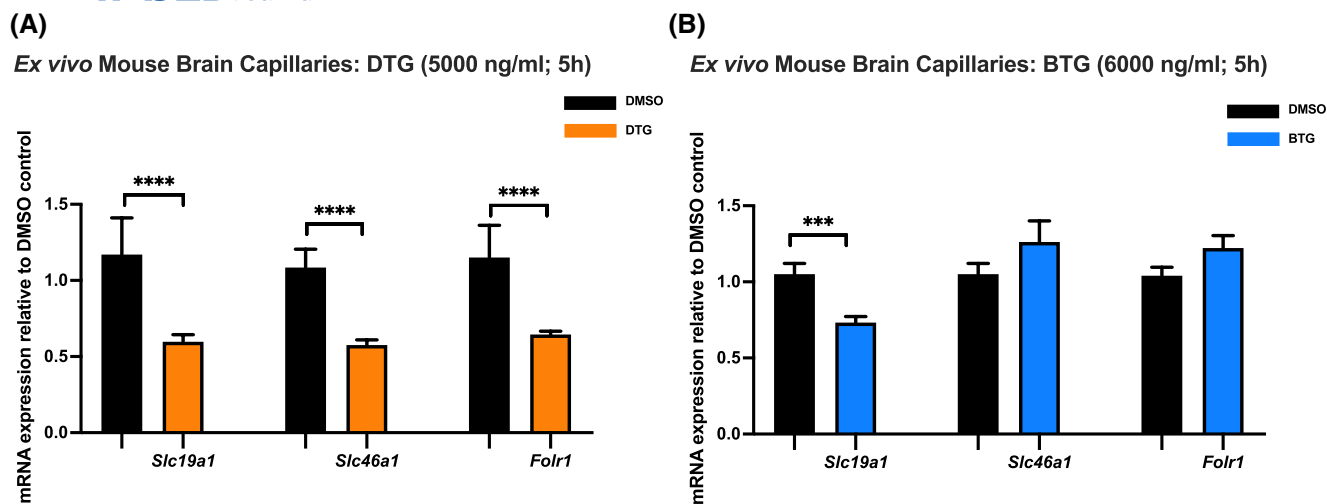
(A) INSTI treated primary cultures of mouse brain microvascular endothelial cells mRNA expression (24h)

(B) INSTI treated primary cultures of mouse brain microvascular endothelial cells protein expression (48h)

FIGURE 2 mRNA and protein expression of folate transporters in primary cultures of mouse brain microvascular endothelial cells exposed to DTG (2000 ng/mL, 5000 ng/mL) or BTG (3000 ng/mL, 6000 ng/mL) or vehicle (DMSO) control for 24 h or 48 h. (A) mRNA expression of *Slc19a1* and *Slc46a1* in mouse cells exposed to INSTIs relative to vehicle (DMSO) control was assessed by qPCR. Results are presented as mean relative mRNA expression ± SEM normalized to the housekeeping mouse cyclophilin B gene from $n = 4$ independent experiments. (B) Protein expression of Rfc and Pcft was assessed by immunoblotting analysis, using specific antibodies as described in the methods section. β-Actin was used as a loading control. Representative blots and densitometric analysis are shown. Results are presented as mean relative protein expression ± SEM normalized to the DMSO control from $n = 3$ independent experiments. One-way ANOVA with Bonferroni's post-hoc test analysis was applied, $*p < .05$; $***p < .01$.

3.6 | Effects of ARVs on pro-inflammatory cytokines and chemokines in vitro in primary cultures of mouse brain microvascular endothelial cells

To examine the effect of first line INSTIs on inflammatory responses at the BBB in vitro, primary cultures of mouse brain microvascular endothelial cells were exposed to DTG (2000 ng/mL or 5000 ng/mL) or BTG (3000 ng/mL or 6000 ng/mL) for 24 h. The gene expressions of pro-inflammatory cytokines *Cxcl1* (~4 fold) and *Cxcl3* (~2.2 fold) were moderately but significantly induced by DTG at 5000 ng/mL but not 2000 ng/mL. However, a significant and robust upregulation of Cxcl2

(A)

Ex vivo Mouse Brain Capillaries: DTG (5000 ng/ml; 5h)

(B)

Ex vivo Mouse Brain Capillaries: BTG (6000 ng/ml; 5h)

FIGURE 3 mRNA expression of folate transporters/receptor in isolated mouse brain capillaries treated ex-vivo for 5 h with DTG (5000 ng/mL) (A) or BTG (6000 ng/mL) (B) relative to vehicle (DMSO) was assessed by qPCR. Results are presented as mean relative mRNA expression ± SEM normalized to the housekeeping mouse cyclophilin B gene from three independent capillary preparation experiments, where each experiment contained brain capillaries pooled from 6 animals per group (total $n = 18$, 3 pools of 6 subjects). Unpaired two-tailed Student's t-test analysis was applied, ***$p < .001$; ****$p < .0001$.

(A)   CP isolated from INSTI treated mice: folate transporters/receptor

(B)   Brain Capillaries isolated from INSTI treated mice: folate transporters/receptor
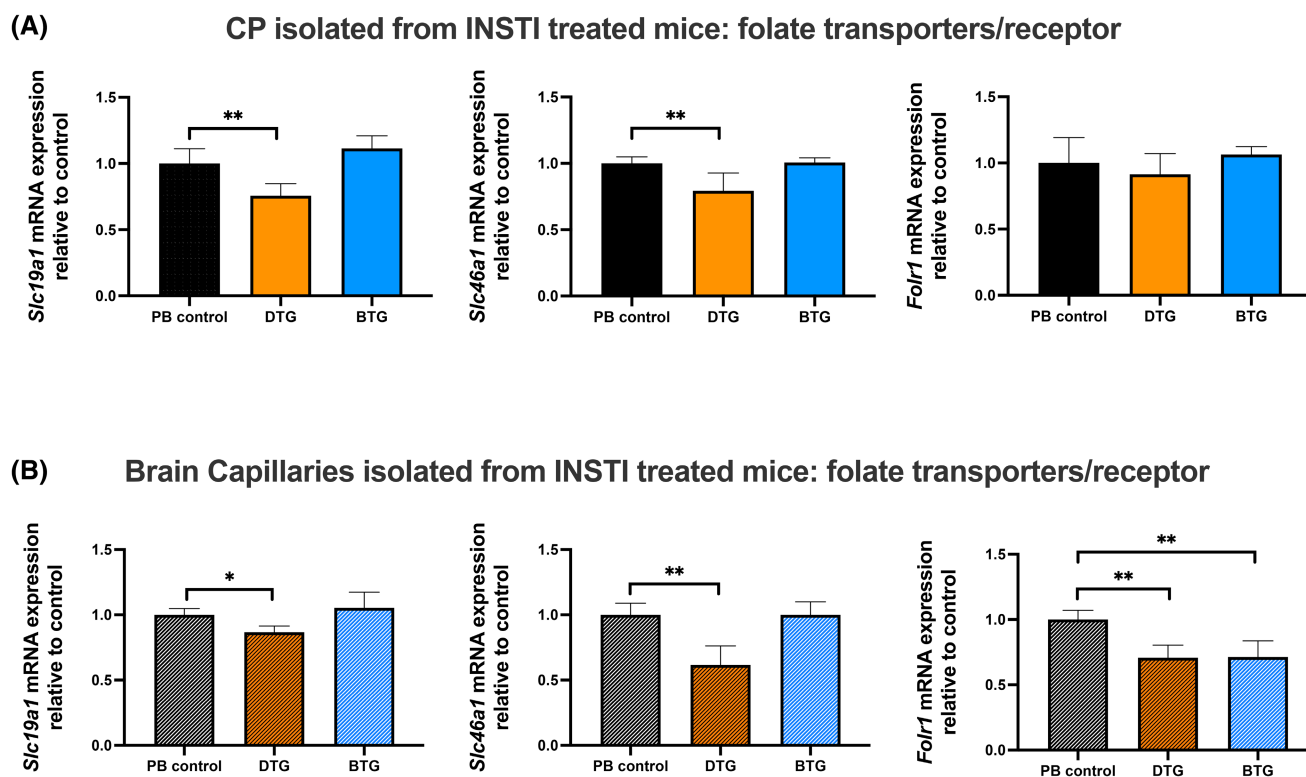
FIGURE 4 mRNA expression of folate transporters/receptor in mouse CP tissues (A) or brain capillaries (B) isolated from mice orally treated with DTG (5 mg/kg/day), BTG (5 mg/kg/day) or vehicle control (PB pellet) for 14 days. The mRNA expression of *Slc19a1, Slc46a1* and *Folr1* genes was assessed by qPCR. Results are presented as mean relative mRNA expression ± SEM from two independent tissue preparations that are normalized to the housekeeping mouse *Gapdh* and cyclophilin B genes for CP tissues (total $n = 12$, 4 pools of 3 subjects) and brain capillaries (total $n = 12$, 2 pools of 6 subjects), respectively. One-way ANOVA with Bonferroni's post-hoc test analysis was applied, *$p < .05$; **$p < .01$.

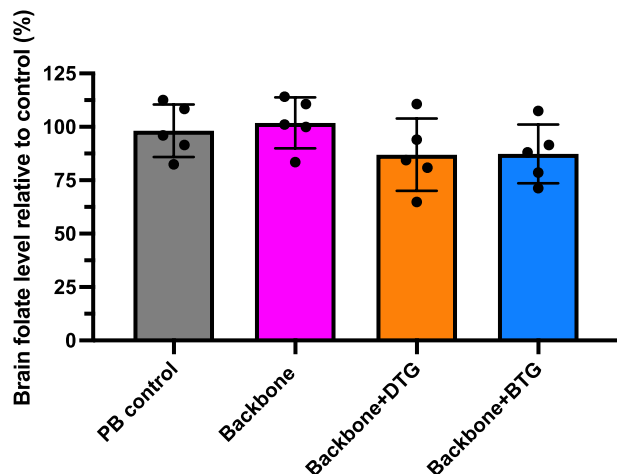**Brain folate quantification (microbiological assay)**

FIGURE 5 Quantification of folate levels in brain tissues of mice treated orally with ARVs. Mice were treated for 14 days with either vehicle (regular PB pellet), or backbone, TAF/FTC (5/33.3 mg/kg/day), or DTG + TAF/FTC (5 + 5/33.3 mg/kg/day), or BTG + TAF/FTC (5 + 5/33.3 mg/kg/day). Folate levels were quantified by a microbiological assay as described in Methods. Data are presented for each individual animal and are expressed as fold change compared to vehicle control, $n = 5$ per group. One-way ANOVA with Bonferroni's post-hoc test analysis was applied.

(~20 fold) gene expression was observed with DTG exposure at 5000 ng/mL. Similarly, DTG treatment at 5000 ng/mL but not 2000 ng/mL strongly induced the gene expression of pro-inflammatory cytokines *Il6* (~15 fold), *Il23a* (~65 fold) and *Il12b* (~40 fold) after 24 h. In contrast, BTG treatment at therapeutic concentrations did not significantly induce the mRNA expression of any pro-inflammatory cytokines or chemokines examined (Figure 6A). Based on the mRNA expression data, pro-inflammatory markers depicting significant changes (Il6, Il12, Il23, Cxcl2) were further selected for ELISA analysis. Our ELISA data showed that DTG treatment at 2000 ng/mL did not significantly alter Il6, Il23 or Cxcl2 content in the cell culture supernatant when compared to DMSO control, with a mild but significant increase of Il12 (~3 pg/mL; ~1.5 fold compared to DMSO control) observed after 24 h. DTG at 5000 ng/mL mildly upregulated Il12 (3.5 pg/mL; ~1.7 fold), but robustly induced Il6 (~3000 pg/mL; ~100 fold), Il23 (~250 pg/mL; ~10 fold), and Cxcl2 (~650 pg/mL; ~6 fold) content compared to DMSO control. As expected, BTG treatment did not significantly alter the levels of any pro-inflammatory markers in the cell culture supernatant, except for a very modest but significant change of Il12 (2.5 pg/mL; ~1.3 fold) (Figure 6B).

3.7 | Effects of chronic exposure of DTG and BTG in vivo on inflammatory cytokines and chemokines expression at the CP isolated from C57BL/6 mice

To investigate potential INSTIs-triggered inflammatory responses at the CP epithelium, we next sought to quantify the mRNA expression of proinflammatory cytokines (*Il6, Il1β, Tnfα*), oxidative stress marker (*Nos2*) and chemokines (*Ccl2, Cxcl1, Cxcl2*) in vivo. We observed a significant upregulation of *Il6* (~2.5 fold), *Tnfα* (~5 fold), and a robust induction of *Il1β* (~11 fold) and *Ccl2* (~14 fold) mRNA expression following DTG treatment. BTG also significantly upregulated the mRNA expression of *Il6* (~1.5 fold), *Il1β* (~2 fold), *Ccl2* (~3 fold) and *Tnfα* (~2.5 fold), but to a much milder level as compared to DTG. The mRNA expression of *Cxcl1, Cxcl2, Nos2* was not detected in any samples (Figure 7).

3.8 | Effects of chronic exposure of DTG and BTG in vivo on ABC transporters expression at the CP and brain capillaries isolated from C57BL/6 mice

To further investigate whether INSTIs dysregulate ABC transporters, the mRNA expression of two highly expressed efflux transporters (*Abcc1, Abcc4*) at the CP was quantified at both CP and brain capillaries. *Abcb1a* and *Abcg2* mRNA expression was additionally assessed at the CP. DTG treatment elicited a downregulatory effect on the mRNA expression of ABC transporters including *Abcc1* (~20%), *Abcc4* (~40%) and *Abcb1a* (~70%) at the CP, while BTG decreased *Abcc4* mRNA expression (~40%) without significantly affecting *Abcc1* or *Abcb1a* mRNA expression. Neither DTG nor BTG significantly affected the mRNA expression of *Abcg2* at the CP (Figure 8A). In contrast within brain capillaries, we observed a robust and significant decrease of *Abcc1* mRNA expression by both DTG (~50%) and BTG (~55%), and a modest but significant downregulation of *Abcc4* mRNA expression by DTG (~20%) and BTG (~20%) (Figure 8B).

3.9 | Effects of chronic exposure of DTG and BTG in vivo on TJ proteins expression at the CP isolated from C57BL/6 mice

To investigate whether INSTIs have any effect on the integrity of CP, we then quantified the mRNA expression of TJ proteins at the CP following DTG and BTG treatment
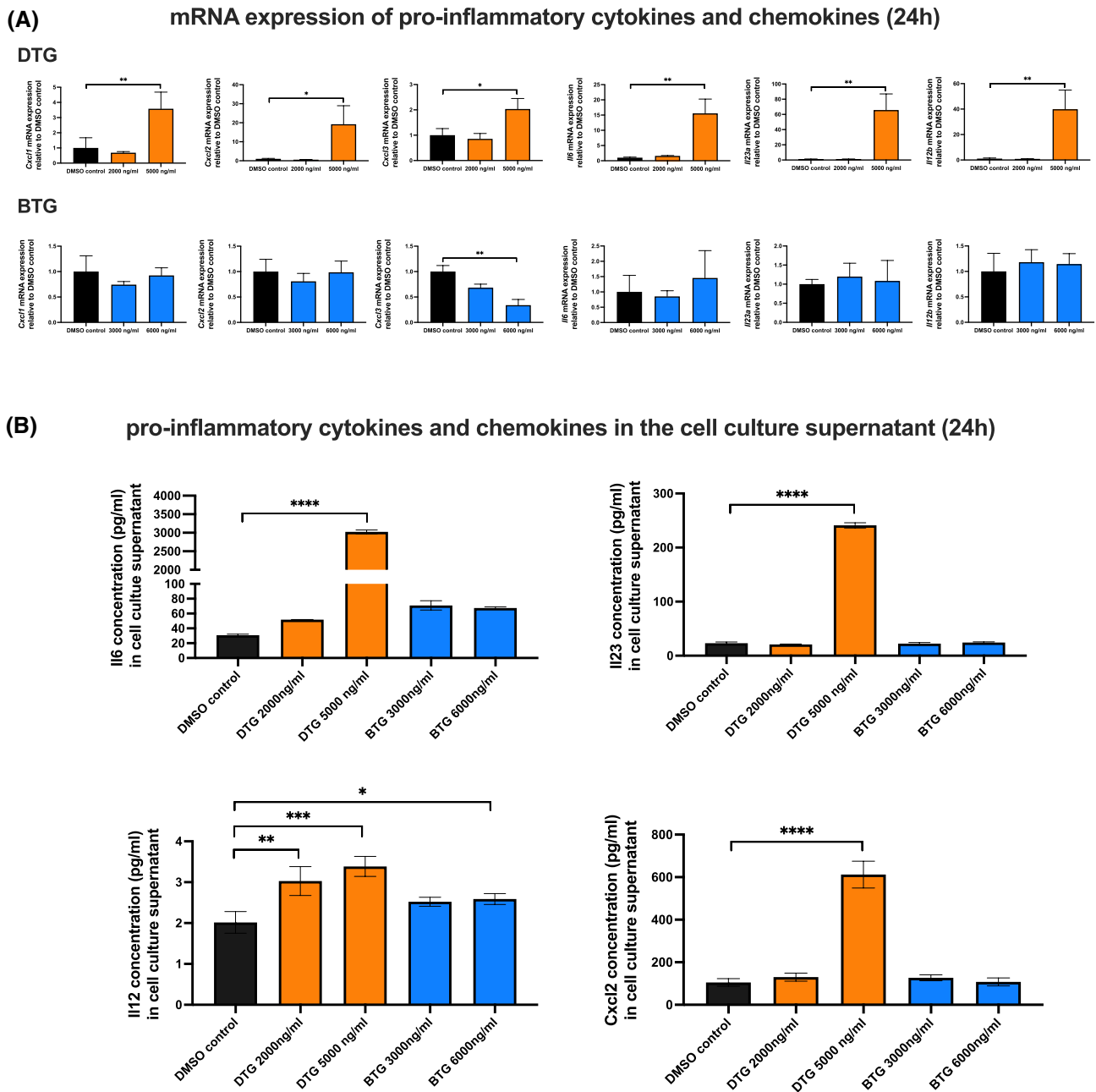
FIGURE 6 mRNA and protein expression of pro-inflammatory cytokines and chemokines in primary cultures of mouse brain microvascular endothelial cells exposed to DTG (2000 ng/mL, 5000 ng/mL) or BTG (3000 ng/mL, 6000 ng/mL) or vehicle (DMSO) control for 24 h. (A) mRNA expression of *Cxcl1, Cxcl2, Cxcl3, Il6, Il23a* and *Il12b* in cells exposed to INSTIs relative to vehicle (DMSO) control was assessed by qPCR. Results are presented as mean relative mRNA expression $\pm$ SEM normalized to the housekeeping mouse cyclophilin B gene from $n = 4$ independent experiments. (B) Protein expression of Il6, Il23, Il12, and Cxcl2 in the cell culture supernatants was assessed by ELISA in cells exposed to INSTIs or vehicle (DMSO) control. Results are presented as the mean value of cytokines and chemokines $\pm$ SEM from $n = 3$ independent experiments. One-way ANOVA with Bonferroni's post-hoc test analysis was applied, *$p < .05$; **$p < .01$; ***$p < .001$; ****$p < .0001$.

in vivo. Neither DTG nor BTG had any significant effect on *Tjp1, Ocln,* or *Cldn1* mRNA expression. However, *Cldn3* mRNA expression was modestly but significantly downregulated by both DTG (~20%) and BTG (~20%) at the CP (Figure 9).

4 | DISCUSSION

Despite the great efficacy of contemporary INSTI – based ART, CNS complications remain a concern among PLWH receiving such pharmacotherapy.[2] Consistent

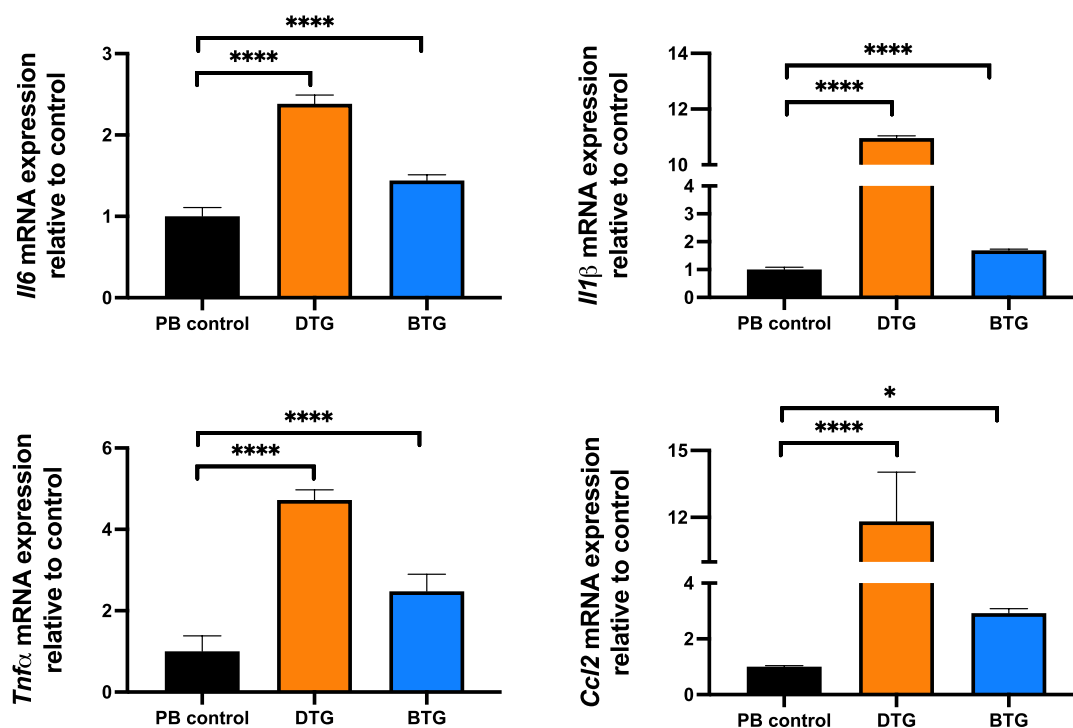## CP isolated from INSTI treated mice: inflammatory markers

FIGURE 7 mRNA expression of inflammatory cytokines and chemokine in mouse CP isolated from mice orally treated with DTG (5 mg/kg/day), BTG (5 mg/kg/day) or vehicle control (PB pellet) for 14 days. The mRNA expression of *Il6, Il1β, Tnfα* and *Ccl2* genes was assessed by qPCR. Results are presented as mean relative mRNA expression $\pm$ SEM from two independent CP tissue preparations (total $n = 12$, 4 pools of 3 subjects) that are normalized to the housekeeping mouse *Gapdh* gene. One-way ANOVA with Bonferroni's post-hoc test analysis was applied, $*p < .05$; $****p < .0001$.

with this, HIV+ individuals appear susceptible to folate deficiency, with such incidence being highest among those exhibiting neuropsychiatric symptoms.[5,54] In 2018, the Tsepamo study documented an increased risk of NTD among HIV+ pregnant women who were pre-conceptionally exposed to DTG.[8] Subsequently several pre-clinical studies identified a potential inhibitory effect of DTG on folate transport at the placental-fetal barrier as a potential explanation.[9,10] Due to the similar manifestation of INSTIs-associated CNS complications and the CFD, we hypothesized that the use of DTG may elicit an inhibitory effect on cerebral folate delivery pathways, which could contribute to the pathogenesis of INSTIs-related NPAEs. In this context, inflammatory response has been suggested to be an important element of cerebral folate levels dysregulation. Consistent with this, elevated pro-inflammatory markers in the CSF are commonly reported in the clinic in association with decreased folate levels in the CSF.[16,18] Pre-clinical studies from our group have indeed reported inflammatory and oxidative stress responses in the context of folate deficiency, documenting elevated pro-inflammatory cytokines and chemokines in primary cultures of mouse

mixed microglial and astrocytes and mouse brain tissues exposed to folate deficient conditions.[17] Thus, this study aimed to assess the effects of DTG on the cerebral folate delivery pathways as well as DTG potential induced inflammatory responses.

Cerebral folate delivery actively occurs at two major blood–brain interfaces, the BCSFB and the BBB. The CP representing the BCSFB, primarily mediates cerebral folate delivery by the concerted effect of FRα and PCFT expressed by the CP epithelial cells.[19,23] In addition, CP is responsible for the production of 60%–75% of the total CSF.[55] Due to its specialized structure and secretory role, the CP is considered as one of the immunological niches in the CNS and plays an important role in relaying inflammatory signaling to the brain parenchyma upon immune activation.[31,38] In recent years multiple studies reported a toxic effect of ARVs in the CNS particularly at the BBB and neurons.[56] Due to the lack of robust in vitro models of CP epithelium, little is known about the effect of ARVs at the CP. To address this challenge, we used CP tissues isolated from mice orally treated with INSTIs yielding clinical therapeutic plasma concentrations[51] to examine potential INSTIs-induced toxicity at the CP.

(A)

CP isolated from INSTI treated mice: ABC transporters

(B)

Brain Capillaries isolated from INSTI treated mice: ABC transporters
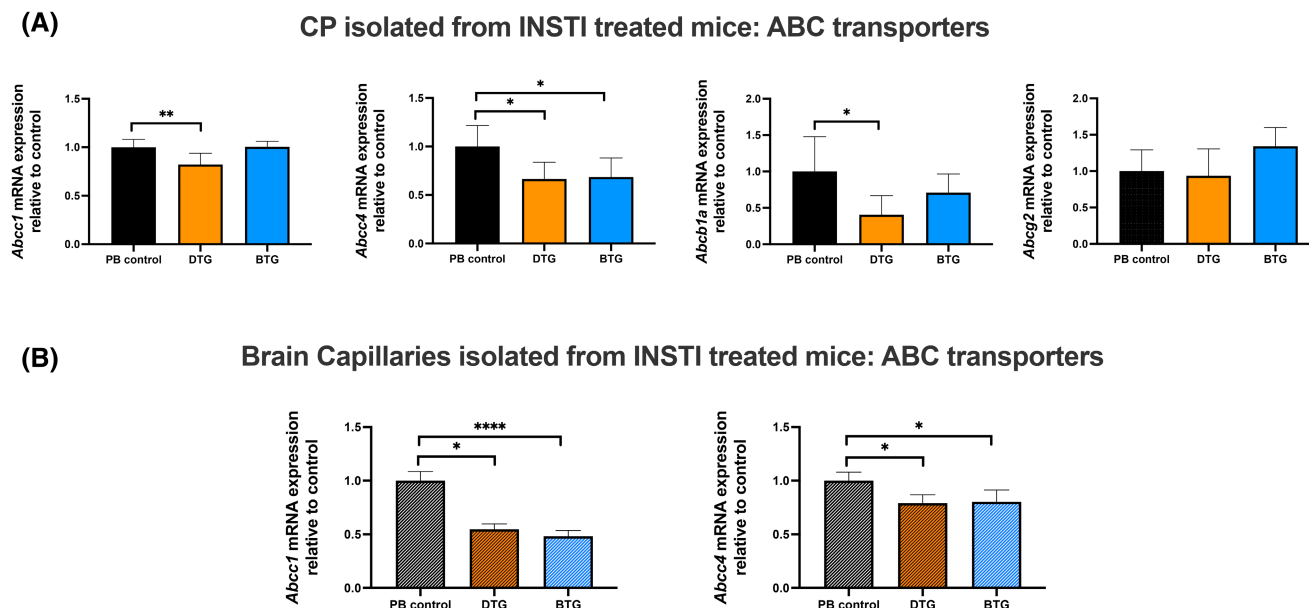

FIGURE 8 mRNA expression of ABC transporters in mouse CP tissues (A) or brain capillaries (B) isolated from mice orally treated with DTG (5 mg/kg/day), BTG (5 mg/kg/day) or vehicle control (PB pellet) for 14 days. The mRNA expression of *Abcc1*, *Abcc4*, *Abcb1a* and *Abcg2* genes was assessed by qPCR. Results are presented as mean relative mRNA expression ± SEM from two independent tissue preparations that are normalized to the housekeeping mouse *Gapdh* and cyclophilin B genes for CP tissues (total $n = 12$, 4 pools of 3 subjects) and brain capillaries (total $n = 12$, 2 pools of 6 subjects), respectively. One-way ANOVA with Bonferroni's post-hoc test analysis was applied, $*p < .05$; $**p < .01$; $****p < .0001$.

CP isolated from INSTI treated mice: TJ proteins
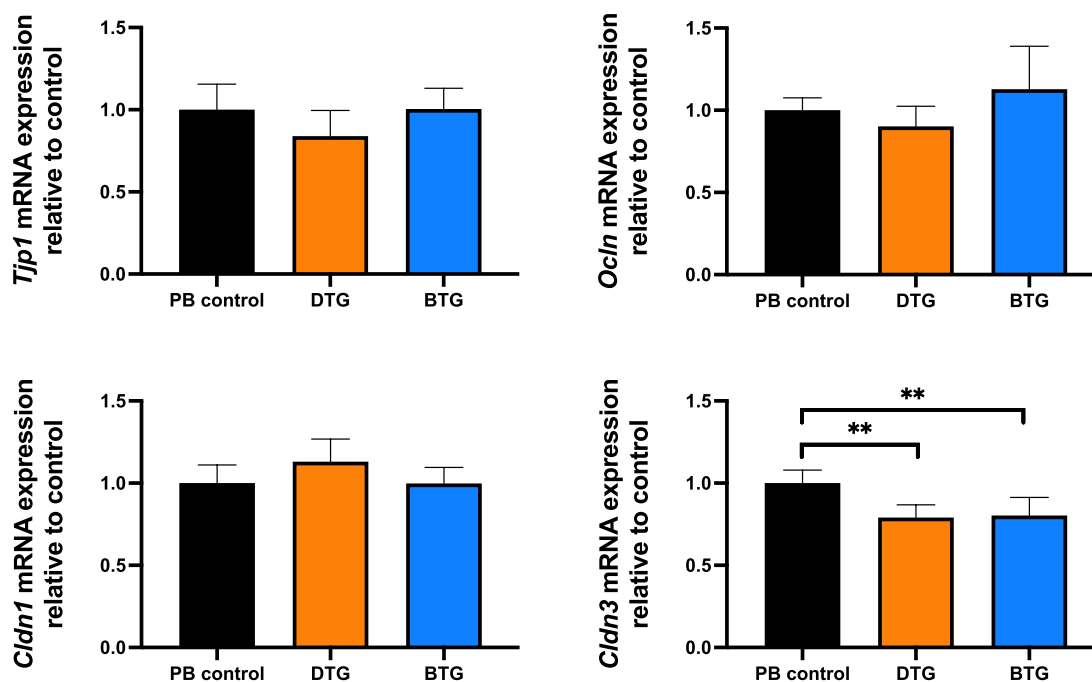
FIGURE 9 mRNA expression of TJ proteins in mouse CP isolated from mice orally treated with DTG (5 mg/kg/day), BTG (5 mg/kg/day) or vehicle control (PB pellet) for 14 days. The mRNA expression of *Tjp1, Ocln, Cldn1* and *Cldn3* genes was assessed by qPCR. Results are presented as mean relative mRNA expression ± SEM from two independent CP tissue preparations (total $n = 12$, 4 pools of 3 subjects) that are normalized to the housekeeping mouse *Gapdh* gene. One-way ANOVA with Bonferroni's post-hoc test analysis was applied, $**p < .01$.

Apart from CP, the cerebral vascular endothelium (BBB) serves as another route for brain folate delivery.[20,57] Clinical reports showed patients presenting mild neurological deficits with FRα and PCFT mutations at the CP epithelium, suggesting that folate uptake effectively occurs at the BBB.[25] Due to the absence of FRα at the human BBB according to the human proteomics data, RFC and PCFT are suggested to be the major players in the folate transport at the human BBB.[58] Like the BCSFB, the BBB also plays a crucial role in the context of brain inflammation.[59] The brain microvascular endothelial cells and associated perivascular cells release pro-inflammatory cytokines and chemokines in response to immune activation, facilitating the trafficking of immune cells and aggravating the neuroinflammation.[60] BBB-related inflammatory response is widely implicated in multiple neurological diseases including HAND.[61] To provide a comprehensive understanding of INSTIs-induced changes on cerebral folate transport pathways and inflammatory response, we then examined the effect of INSTIs at the BBB using in vitro human and mouse BBB models, ex vivo and in vivo isolated mouse brain capillaries.

Our in vitro, ex vivo, and in vivo data reveal consistent downregulation of *Slc19a1* (Rfc) and *Slc46a1* (Pcft) expression at the mouse BBB treated with DTG, two major transporters in regulating folate at the human BBB. Immunoblotting data further confirm that DTG downregulates PCFT/Pcft and RFC/Rfc protein expression in hCMEC/D3 cells and primary cultures of mouse brain microvascular endothelial cells at clinically relevant concentrations. These data corroborate previous findings from our group demonstrating an inhibitory effect of DTG on mRNA/protein expression of RFC and PCFT in human placental cells and human placental tissue explants.[9,10] Despite its highest affinity, FRα remained unchanged at the CP epithelium in our animal study. Humans with PCFT mutations also present neurological deficits due to CFD.[15] Therefore the downregulated Pcft expression observed in DTG-treated mice at the CP is likely to affect cerebral folate delivery by hindering folate export from exosomes in the CSF and/or from acidified endosomes within the CP epithelium.[21] However, our second in vivo study quantifying brain folate levels did not reveal any significant changes in any of the C57BL/6 mice groups following 14-day treatment. This could most likely be related to the absence of major changes in the expression of Frα. However other explanations remain possible including: (i) the high folate level in the brain compared to plasma,[37] which makes it difficult to identify potential mild changes induced by ARVs, (ii) the 14-day treatment period, which may have not been sufficiently long to induce changes in cerebral folate levels, and/or (iii) the small number of animals used per group ($n = 5$), which limits the generation of potential statistical significance.

Due to the pivotal roles of the two major blood–brain interfaces (BCSFB and BBB) in relaying inflammatory signals in the brain, we examined the effects of DTG and BTG on pro-inflammatory cytokine and chemokine expression at these barriers. This study demonstrates that DTG but not BTG robustly induced the mRNA expression of pro-inflammatory cytokines (*Il6, Il23a, Il12b*) and chemokines (*Cxcl1, Cxcl2, Cxcl3*) in primary cultures of mouse brain microvascular endothelial cells. The ELISA analyses based upon release from cell culture supernatants are in general agreement with that derived from mRNA data, demonstrating that DTG (5000 ng/mL) but not BTG treatment robustly induced the expression of pro-inflammatory cytokines and chemokines (*Il6, Il12, Il23 Cxcl2*) in the cell culture supernatants after 24 h exposure to the INSTIs. Our data are in agreement with our recent published data demonstrating that DTG but not BTG induced an inflammatory response in in vitro human and mouse BBB models.[43] In parallel to the BBB, our data showed that at the CP, a 14-day treatment of DTG in C57BL/6 mice also resulted in a significantly robust elevation of pro-inflammatory cytokines and chemokines (*Il6, Il1β, Tnfα* and *Ccl2*), whereas BTG exhibited a modest effect. Notably, due to the extensive cell–cell communication at the CP, studies on inflammatory response at the BCSFB are generally limited. To overcome this challenge, we herein directly isolated CP tissues from the animals treated with DTG or BTG where cell–cell communication such as leukocyte recruitment could actively occur.[62]

Mrp1 and Mrp4 are the two major efflux transporters localized to the basolateral membrane of CP epithelial cells, facilitating CSF-to-blood transport, and limiting the drug entry from the systemic circulation into the CSF.[63] Notably, Mrp1 and Mrp4 are also expressed at the basolateral side of BBB in both human and rodents, and responsible for the brain-to-blood transport of xenobiotics.[64] The dysregulation of membrane transporters at both brain barriers can result in an alteration of drug disposition in the CSF and brain.[63] In our study, we demonstrated that the chronic treatment of DTG in vivo significantly downregulated the gene expression of efflux transporters *Abcc1* and *Abcc4* at both the CP and brain capillaries. Although a downregulatory effect of *Abcc4* but not *Abcc1* gene expression was also observed with BTG treatment, the change was milder compared to DTG. Our findings corroborate the data from our recent study, which demonstrated that DTG had a greater effect than BTG in dysregulating membrane associated transporters (P-gp, Bcrp) at the mouse BBB *in vitro, ex vivo,* and in vivo.[43] Additionally, we demonstrated in this study that DTG treatment in vivo significantly downregulated the gene expression of *Abcb1a*

(P-gp) at the CP, which also corroborates our recent study showing a downregulatory effect of both DTG and BTG on *Abcb1a* and *Abcg2* gene expression at the brain capillaries in C57BL/6 mice.[43]

In addition to the ABC membrane associated transporters, the barrier function of BCSFB is also highly regulated by TJ proteins expressed within the CP.[65] In the context of HIV infection, disruption in BCSFB could provide a facilitated path for viral invasion.[66] In this study, we found a modest downregulation in *Cldn3* gene expression at the CP by both DTG and BTG *in vivo,* which is in agreement with our previous results demonstrating a downregulation of TJ proteins (Zo-1, Ocln and Cldn5) in the BBB models used.[43] However, considering the modest change, whether this effect leads to a BCSFB leakiness needs to be further assessed.

Taken together, these data demonstrate for the first-time that DTG but not BTG induced an inflammatory response in a rodent BBB and BCSFB model. A 14 day-DTG oral treatment in rodents downregulated the gene expression of folate transporters/receptor at both brain barriers. Despite this, such changes did not alter brain folate levels in the animals. Despite the chemical structural similarities, observed toxic effects were generally minor with BTG treatment compared to DTG at both the BCSFB and BBB. It is worth noting that, despite the unchanged brain folate level in this animal study, the potential inhibitory effects of DTG on brain folate transport may become more prominent among PLWH due to their susceptibility to folate deficiency. Nonetheless, it is important to address the limitations of our study. Due to the low yield of CP and brain capillaries, the protein expression of folate transporters/receptor, TJ proteins, ABC membrane associated transporters, as well as pro-inflammatory markers could not be examined. Additionally, the observed changes in the expression of our markers may not only occur in the brain microvascular endothelial cells but may also reflect changes in other non-endothelial cell populations (e.g., pericytes and astrocytes) which are important components of the BBB and where folate transporters are known to be expressed.[27] However, our current data provide valuable insights into the context of ARV toxicity which can potentially contribute to ARV-related NPAEs.

5 | CONCLUSION

This study demonstrates that DTG but not BTG significantly induced an inflammatory response in a rodent BCSFB and BBB model. These findings provide valuable insights in the mechanism of DTG-induced brain toxicity, which could potentially contribute to the high incidence of NPAEs associated with the clinical use of DTG-based

ART. Considering the high incidence of CNS complications among PLWH on INSTI-based ART, additional research is needed to examine the CNS toxicities of first line ARVs, and their underlying mechanisms.

AUTHOR CONTRIBUTIONS

CH, QRQ, and MTH performed the experimental work, JH performed CP tissue isolation and edited manuscript, and CH, QRQ, MTH, and RB verified the underlying data. RB conceived the study and directed the research. CH, MTH, and RB drafted the manuscript. All authors have read and approved the final version of the manuscript.

DATA AVAILABILITY STATEMENT

Included in article. The data that support the findings of this study are available in the Materials and Methods, Results, and/or Supplemental Material of this article.

ORCID

Chang Huang https://orcid.org/0009-0002-6622-8959
Md. Tozammel Hoque https://orcid.org/0000-0003-4802-0257
Qing Rui Qu https://orcid.org/0009-0008-4938-5745
Jeffrey Henderson https://orcid.org/0000-0001-7636-2604
Reina Bendayan https://orcid.org/0000-0002-0145-881X

REFERENCES

1. Clifford DB. HIV-associated neurocognitive disorder. *Curr Opin Infect Dis*. 2017;30(1):117-122.

2. Cailhol J, Rouyer C, Alloui C, Jeantils V. Dolutegravir and neuropsychiatric adverse events: a continuing debate. *AIDS*. 2017;31(14):2023-2024.

3. Robertson KR, Su Z, Margolis DM, et al. Neurocognitive effects of treatment interruption in stable HIV-positive patients in an observational cohort. *Neurology*. 2010;74(16):1260-1266.

4. Buell KG, Chung C, Chaudhry Z, Puri A, Nawab K, Ravindran RP. Lifelong antiretroviral therapy or HIV cure: the benefits for the individual patient. *AIDS Care*. 2016;28(2):242-246.

5. Lefevre G. Altered folate metabolism in early HIV infection. *JAMA J Am Med Assoc*. 1988;259(21):3128-3129.

6. Estill J, Bertisch B. More evidence for dolutegravir as first-line ART for all. *Lancet HIV*. 2020;7(3):e154-e155.

7. De Boer MGJ, Van Den Berk GEL, Van Holten N, et al. Intolerance of dolutegravir-containing combination antiretroviral therapy regimens in real-life clinical practice. *AIDS*. 2016;30(18):2831-2834.

8. Zash R, Makhema J, Shapiro RL. Neural-tube defects with dolutegravir treatment from the time of conception. *N Engl J Med*. 2018;379(10):979-981.

9. Gilmore JC, Hoque MT, Dai W, et al. Interaction between dolutegravir and folate transporters and receptor in human and rodent placenta. *EBioMedicine*. 2022;75:103771.

10. Mohan H, Lenis MG, Laurette EY, et al. Dolutegravir in pregnant mice is associated with increased rates of fetal defects at therapeutic but not at supratherapeutic levels. *EBioMedicine*. 2021;63:103167.

11. Ducker GS, Rabinowitz JD. One-carbon metabolism in health and disease. *Cell Metab*. 2017;25(1):27-42.

12. McGarel C, Pentieva K, Strain JJ, McNulty H. Emerging roles for folate and related B-vitamins in brain health across the lifecycle. *Proc Nutr Soc*. 2015;74(1):46-55.

13. Pope S, Artuch R, Heales S, Rahman S. Cerebral folate deficiency: analytical tests and differential diagnosis. *J Inherit Metab Dis*. 2019;42(4):655-672.

14. Bottiglieri T. Folate, vitamin B12, and neuropsychiatric disorders. *Nutr Rev*. 2009;54(12):382-390.

15. Ramaekers VT, Quadros EV. Cerebral folate deficiency syndrome: early diagnosis, intervention and treatment strategies. *Nutrients*. 2022;14(15):3096.

16. Hasselmann O, Blau N, Ramaekers VT, Quadros EV, Sequeira JM, Weissert M. Cerebral folate deficiency and CNS inflammatory markers in Alpers disease. *Mol Genet Metab*. 2010;99(1):58-61.

17. Sangha V, Aboulhassane S, Qu QR, Bendayan R. Protective effects of pyrroloquinoline quinone in brain folate deficiency. *Fluids Barriers CNS*. 2023;20(1):84.

18. Rossignol DA, Frye RE. A review of research trends in physiological abnormalities in autism spectrum disorders: immune dysregulation, inflammation, oxidative stress, mitochondrial dysfunction and environmental toxicant exposures. *Mol Psychiatry*. 2012;17(4):389-401.

19. Alam C, Hoque MT, Sangha V, Bendayan R. Nuclear respiratory factor 1 (NRF-1) upregulates the expression and function of reduced folate carrier (RFC) at the blood-brain barrier. *FASEB J*. 2020;34(8):10516-10530.

20. Araújo JR, Gonçalves P, Martel F. Characterization of uptake of folates by rat and human blood-brain barrier endothelial cells. *Biofactors*. 2010;36(3):201-209.

21. Grapp M, Wrede A, Schweizer M, et al. Choroid plexus transcytosis and exosome shuttling deliver folate into brain parenchyma. *Nat Commun*. 2013;4(1):2123.

22. Wollack JB, Makori B, Ahlawat S, et al. Characterization of folate uptake by choroid plexus epithelial cells in a rat primary culture model: folate transport by choroid epithelial cells. *J Neurochem*. 2008;104(6):1494-1503.

23. Zhao R, Min SH, Wang Y, Campanella E, Low PS, Goldman ID. A role for the proton-coupled folate transporter (PCFT-SLC46A1) in folate receptor-mediated endocytosis. *J Biol Chem*. 2009;284(7):4267-4274.

24. Zhao R, Aluri S, Goldman ID. The proton-coupled folate transporter (PCFT-SLC46A1) and the syndrome of systemic and cerebral folate deficiency of infancy: hereditary folate malabsorption. *Mol Asp Med*. 2017;53:57-72.

25. Wang Y, Zhao R, Russell RG, Goldman ID. Localization of the murine reduced folate carrier as assessed by immunohistochemical analysis. *Biochim Biophys Acta Biomembr*. 2001;1513(1):49-54.

26. Alam C, Aufreiter S, Georgiou CJ, et al. Upregulation of reduced folate carrier by vitamin D enhances brain folate uptake in mice lacking folate receptor alpha. *Proc Natl Acad Sci*. 2019;116(35):17531-17540.

27. Sangha V, Hoque MT, Henderson JT, Bendayan R. Novel localization of folate transport systems in the murine central nervous system. *Fluids Barriers CNS*. 2022;19(1):92.

28. Wang X, Cabrera RM, Li Y, Miller DS, Finnell RH. Functional regulation of P-glycoprotein at the blood-brain barrier in proton-coupled folate transporter (PCFT) mutant mice. *FASEB J*. 2013;27(3):1167-1175.

29. Wu D, Pardridge WM. Blood-brain barrier transport of reduced folic acid. *Pharm Res*. 1999;16(3):415-419.

30. Liddelow SA. Development of the choroid plexus and blood-CSF barrier. *Front Neurosci*. 2015;9:32.

31. Thompson D, Brissette CA, Watt JA. The choroid plexus and its role in the pathogenesis of neurological infections. *Fluids Barriers CNS*. 2022;19(1):75.

32. Shin K, Fogg VC, Margolis B. Tight junctions and cell polarity. *Annu Rev Cell Dev Biol*. 2006;22(1):207-235.

33. Morris ME, Rodriguez-Cruz V, Felmlee MA. SLC and ABC transporters: expression, localization, and species differences at the blood-brain and the blood-cerebrospinal fluid barriers. *AAPS J*. 2017;19(5):1317-1331.

34. Tachikawa M, Watanabe M, Hori S, et al. Distinct spatiotemporal expression of ABCA and ABCG transporters in the developing and adult mouse brain: ABCA and ABCG transporter mRNAs in the mouse brain. *J Neurochem*. 2005;95(1):294-304.

35. Yasuda K, Cline C, Vogel P, et al. Drug transporters on arachnoid barrier cells contribute to the blood–cerebrospinal fluid barrier. *Drug Metab Dispos*. 2013;41(4):923-931.

36. Cui J, Xu H, Lehtinen MK. Macrophages on the margin: choroid plexus immune responses. *Trends Neurosci*. 2021;44(11):864-875.

37. Spector R, Johanson CE. The nexus of vitamin homeostasis and DNA synthesis and modification in mammalian brain. *Mol Brain*. 2014;7(1):1-9.

38. Strominger I, Elyahu Y, Berner O, et al. The choroid plexus functions as a niche for T-cell stimulation within the central nervous system. *Front Immunol*. 2018;9:1066.

39. Edelblum KL, Turner JR. The tight junction in inflammatory disease: communication breakdown. *Curr Opin Pharmacol.* 2009;9(6):715-720.

40. Ronaldson PT, Bendayan R. HIV-1 viral envelope glycoprotein gp120 triggers an inflammatory response in cultured rat astrocytes and regulates the functional expression of P-glycoprotein. *Mol Pharmacol.* 2006;70(3):1087-1098.

41. Zheng J, Yang P, Dai J, et al. Dynamics of intestinal inflammatory cytokines and tight junction proteins of turbot (*Scophthalmus maximus* L.) during the development and recovery of enteritis induced by dietary β-conglycinin. *Front Mar Sci.* 2020;7:198.

42. Domingo P, Quesada-López T, Villarroya J, et al. Differential effects of dolutegravir, bictegravir and raltegravir in adipokines and inflammation markers on human adipocytes. *Life Sci.* 2022;308:120948.

43. Huang C, Hoque MT, Bendayan R. Antiretroviral drugs efavirenz, dolutegravir and bictegravir dysregulate blood-brain barrier integrity and function. *Front Pharmacol.* 2023;14:1118580.

44. Cabrera RM, Souder JP, Steele JW, et al. The antagonism of folate receptor by dolutegravir: developmental toxicity reduction by supplemental folic acid. *AIDS.* 2019;33(13):1967-1976.

45. Markham A. Bictegravir: first global approval. *Drugs.* 2018;78(5):601-606.

46. Weksler B, Romero IA, Couraud PO. The hCMEC/D3 cell line as a model of the human blood brain barrier. *Fluids Barriers CNS.* 2013;10(1):16.

47. Chan GNY, Cannon RE. Assessment of ex vivo transport function in isolated rodent brain capillaries. *Curr Protoc Pharmacol.* 2017;76(1):7161-7167.

48. Hoque MT, Shah A, More V, Miller DS, Bendayan R. *In vivo* and *ex vivo* regulation of breast cancer resistant protein (Bcrp) by peroxisome proliferator-activated receptor alpha (Pparα) at the blood–brain barrier. *J Neurochem.* 2015;135(6):1113-1122.

49. Elliot E, Amara A, Jackson A, et al. Dolutegravir and elvitegravir plasma concentrations following cessation of drug intake. *J Antimicrob Chemother.* 2016;71(4):1031-1036.

50. Rigo-Bonnin R, Tiraboschi JM, Álvarez-Álvarez M, et al. Measurement of total and unbound bictegravir concentrations in plasma and cerebrospinal fluid by UHPLC-MS/MS. *J Pharm Biomed Anal.* 2020;185:113250.

51. Kala S, Watson B, Zhang JG, et al. Improving the clinical relevance of a mouse pregnancy model of antiretroviral toxicity; a pharmacokinetic dosing-optimization study of current HIV antiretroviral regimens. *Antivir Res.* 2018;159:45-54.

52. Horne DW. Microbiological assay of folates in 96-well microtiter plates. *Methods in Enzymology.* Vol 281. Elsevier; 1997:38-43.

53. Alam C, Hoque MT, Finnell RH, Goldman ID, Bendayan R. Regulation of reduced folate carrier (RFC) by vitamin D receptor at the blood-brain barrier. *Mol Pharm.* 2017;14(11):3848-3858.

54. Adhikari PMR, Chowta M, Ramapuram J, Rao S, Udupa K, Acharya S. Prevalence of vitamin B_{12} and folic acid deficiency in HIV-positive patients and its association with neuropsychiatric symptoms and immunological response. *Indian J Sex Transm Dis AIDS.* 2016;37(2):178-184.

55. Lun MP, Monuki ES, Lehtinen MK. Development and functions of the choroid plexus–cerebrospinal fluid system. *Nat Rev Neurosci.* 2015;16(8):445-457.

56. Lanman T, Letendre S, Ma Q, Bang A, Ellis R. CNS neurotoxicity of antiretrovirals. *J Neuroimmune Pharmacol.* 2021;16(1):130-143.

57. Alam C, Kondo M, O'Connor DL, Bendayan R. Clinical implications of folate transport in the central nervous system. *Trends Pharmacol Sci.* 2020;41(5):349-361.

58. Steinfeld R, Grapp M, Kraetzner R, et al. Folate receptor alpha defect causes cerebral folate transport deficiency: a treatable neurodegenerative disorder associated with disturbed myelin metabolism. *Am J Hum Genet.* 2009;85(3):354-363.

59. Galea I. The blood–brain barrier in systemic infection and inflammation. *Cell Mol Immunol.* 2021;18(11):2489-2501.

60. Takata F, Nakagawa S, Matsumoto J, Dohgu S. Blood-brain barrier dysfunction amplifies the development of neuroinflammation: understanding of cellular events in brain microvascular endothelial cells for prevention and treatment of BBB dysfunction. *Front Cell Neurosci.* 2021;15:661838.

61. Rosenberg GA. Neurological diseases in relation to the blood–brain barrier. *J Cereb Blood Flow Metab.* 2012;32(7):1139-1151.

62. Schwartz M, Baruch K. The resolution of neuroinflammation in neurodegeneration: leukocyte recruitment via the choroid plexus. *EMBO J.* 2014;33(1):7-22.

63. Gazzin S, Strazielle N, Schmitt C, et al. Differential expression of the multidrug resistance-related proteins ABCb1 and ABCc1 between blood-brain interfaces. *J Comp Neurol.* 2008;510(5):497-507.

64. Löscher W, Potschka H. Blood-brain barrier active efflux transporters: ATP-binding cassette gene family. *NeuroRx.* 2005;2(1):86-98.

65. Kratzer I, Ek J, Stolp H. The molecular anatomy and functions of the choroid plexus in healthy and diseased brain. *Biochim Biophys Acta Biomembr.* 2020;1862(11):183430.

66. Hanly A, Petito CK. HLA-DR-positive dendritic cells of the normal human choroid plexus: a potential reservoir of HIV in the central nervous system. *Hum Pathol.* 1998;29(1):88-93.

SUPPORTING INFORMATION

Additional supporting information can be found online in the Supporting Information section at the end of this article.